*Int. Rev. Appl. Sci. Eng. 10 (2019) 2, 173–181*
*DOI: 10.1556/1848.2019.0021*
*First published online: August 1, 2019*

# TRIBOLOGY BEHAVIOUR INVESTIGATION OF 3D PRINTED POLYMERS

*MUAMMEL M. HANON*[1,2,*], *MÁRK KOVÁCS*[3], *LÁSZLÓ ZSIDAI*[3]

[1] Institute for Mechanical Engineering Technology, Mechanical Engineering Doctoral School, Szent István University, 2100 Gödöllő, Hungary
[2] Baquba Technical Institute, Middle Technical University (MTU), Baghdad, Iraq
[3] Institute for Mechanical Engineering Technology, Szent István University, 2100 Gödöllő, Hungary
* E-mail: muammel_mmr_85@yahoo.com, Sharba.Muammel.M.Hanon@phd.uni-szie.hu (Corresponding author)

3D printing of Acrylonitrile Butadiene Styrene (ABS) and Poly Lactic Acid (PLA) were used to prepare specimens utilising fused deposition modelling (FDM) technology. Two colours of PLA filament were printed; white and grey, whereas ABS only in white colour. Determining the tribological properties of 3D printed samples have been carried out, through obtaining the frictional features of different 3D printable filaments. Alternating-motion system employed for measuring the tribological factors. Studying the difference between static and dynamic friction factors and the examination of wear values were included. A comparison among the tribological behaviour of the 3D printed polymers has been investigated. The printed white ABS and PLA specimens show insignificant differences in the results tendency. On the contrary, the grey PLA exhibits a considerable variation due to the incredible growth in the coefficient of friction and wear average as well.

***Keywords:*** *3D printing, friction, wear, PLA, ABS, tribology*

## 1. Introduction

Three-dimensional (3D) printing technology is an additive manufacturing (AM) process that enables the fabrication of objects by adding layers of materials on top of each other successively [1, 2]. Fused deposition modelling (FDM) (alias fused filament fabrication – FFF) is currently the most applied AM technology [3], its printers work by controlled extrusion of thermoplastic polymer filaments to 3D print layers (layer by layer) of materials and then solidify into final parts [4], as shown in Fig. 1. Thermoplastics such as acrylonitrile butadiene styrene (ABS) [5, 6], polycarbonate (PC) [7], and polylactic acid (PLA) [8], are commonly used due to their low melting temperature as well as their diversity and ease of adoption to different 3D printing processes. The capability of employing 3D printing of polymers and composites has been explored for several years in many industrial applications, such as the aerospace, architectural, toy fabrication and medical fields. Ongoing research aimed at resolving the inferior mechanical properties of 3D printed polymers has been conducted, which led to better performance of advanced polymer composites [9].

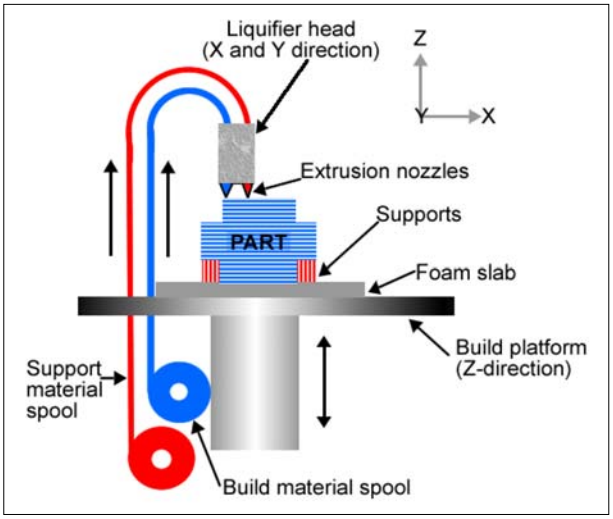


**Fig. 1.** Fused deposition modelling schematic [10]



*ISSN 2062-0810*

Tribology deals with the relative motion of surfaces. It involves friction, wear of materials, scratching and rubbing. A more precise definition describes tribology as a science and technology of surfaces that are in contact and relative motion, as well as supporting activities that should reduce costs resulting from friction and wear [11]. Polymers can be picked as a solution in specific applications of machine construction because of their strength, chemical resistance, and self-lubricating ability [12]. It has been noticed from the literature that widespread interest in plastics has raised in the mid-twentieth century due to the features of their structure, specific mechanical behaviour, and the significant possibility to change the polymer properties.

Consequently, extensive studies over many years have developed in the field of modern engineering in which the plastics can be applied as tribological materials. However, it is apparent to recognise from the literature that there is a lack of research that deals with the tribological characteristics of the 3D printed structure. Therefore, it appears essential to study the tribology of 3D printed polymers in order to grasp the influence of 3D printed structures and surfaces on the tribology behaviours of polymers.

In the present research, 3D printed polymer specimens are produced by the fused deposition modelling (FDM) technology. The frictional properties (under static conditions) and wear rate of 3D printed polymer samples are considered as the fundamental tribological features. As experimental conditions for the 3D printing, different materials (ABS and PLA) and colours (White and grey) of polymer in various printing temperature ranges (Low, opt and max) are applied to lead a regular and overload conditions, in order to estimate the operating range and determine failure modes of the 3D printed polymer samples.

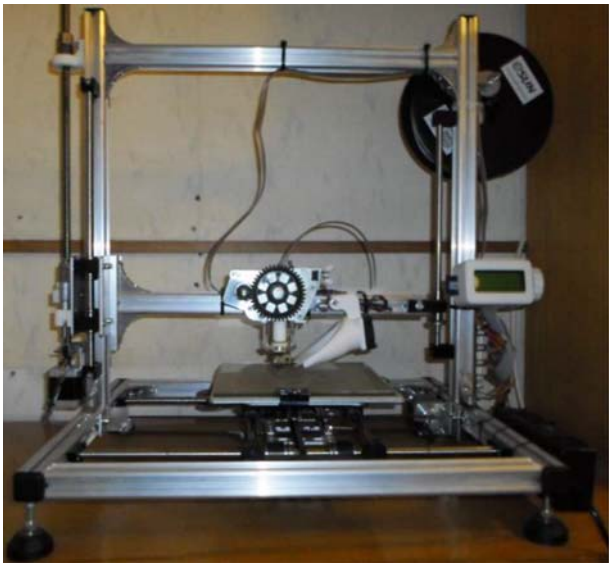

**Fig. 2.** 3D printer K8200

## 2. Materials and methods

### *2.1. 3D printer*

The printed test pieces were made with a 3D printer works according to the Fused Filament Fabrication (FFF) for PLA and ABS, which is the most suitable technology as mentioned in the literature. The model of the used 3D printer is K8200 (Fig. 2).

It can be seen in Fig. 2; the printer consists of a frame structure, extruder, heated work surface, fan, adapter, power supply, filament holder, and controller. The G-Code of the 3D model can be incorporated directly from the SD card. All parameters and commands are given from a computer via USB cable. The model was designed using Solid Edge software. The file has been saved as "stl" format due to its compati-

**Table 1.** Technical specifications of the K8200 printer [13]

| Technology | FFF (Fused Filament Fabrication) |
|---|---|
| Usable materials | PLA and ABS |
| Power supply | 15 V / 6.6 A max |
| Port | USB 2.0 and SD card |
| Dimensions of printable area | 200×200×200 mm |
| Typical printing speeds | 120 mm/s |
| Maximum print speed | 150–300 mm/s (depending on the object to be printed) |
| Extrusion nozzle | 0.5 mm |
| Temperature sensor | NTC 100 K |
| Movement | 3 stepping motor (4NEMA) |
| Rated mechanical resolution | $x$ and $y$: 0.015 mm, $z$: 0.781 µm |
| Nominal printing resolution | Thickness ($x$, $y$): 0.5 mm, Layer thickness: 0.2–0.25 mm |
| Dimensions | Width: 500 mm, Depth: 240 mm, Height: 620 mm |
| Weight | 9 kg |

**Table 2.** Main features of filaments [14]

| Base material of filament | Print temperature [°C] | First layer temperature [°C] | Heated work surface |
|---|---|---|---|
| ABS | 220–260 | 235 | Yes |
| PLA | 190–220 | 195 | Optional |

bility with most slicing programs. For the slicing purpose, K8200 Repetier-Host software was used which is the recommended and prepared for the same printer. The Technical specifications of 3D printer K8200 are listed in Table 1.

*2.2. Preparation of specimens*

The 3D printed test pieces were made from ABS and PLA. Both materials in the form of filament are available in the market, and its key features are presented in Table 2. The two different materials were used to 3D print the test pieces. The test specimens have a diameter of 7.5 mm and a length of 10 mm as seen in Fig. 3.

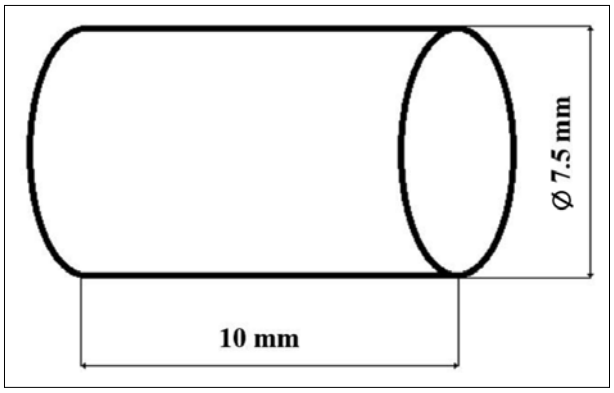


**Fig. 3.** Dimensions of the test specimen

The work table of printing ABS is preheated to approximately 60–70 °C. The work surface is treated for proper adhesion, due to its more delicate for temperature fluctuations than PLA during printing. In case of insufficient cooling during printing, no optimum melting of the layers is reached, and brittle fracture of material takes place. For PLA printing, no pre-treatment of the work surface is required, but it is recommended to preheat the work surface at 40–55 °C for better adhesion. Since this material is less susceptible, therefore, sets of printed pieces have also been produced as an alternative. White and grey filament colours of the PLA material were used in the 3D printing. According to the manufacturer of the used PLA filament, the optimal temperature for printing is 205 °C. Temperature ranges of higher and lower than the optimal were tested in the current work. These ranges are called; low, opt, and max settings. Precisely the temperature range for the low: 190–195 °C, opt: 200–205 °C, and max: 215–220 °C. Five repeated samples have been printed for each colour and specific setting. This implies that the print temperature range for each group is different from other sets. Fig. 4 shows some of the printed workpieces with a colour code.

*2.3. Measurements*

After printing the specimens, the measurements were performed at tribology laboratory of Szent István University under the laboratory conditions. The first step in the measurement process is to connect the measuring circuit, which consists of a computer, Spider 8 measuring converter, a tribotester and, an inverter. The indispensable part of the measuring system is the tribotester, which is in this case compatible with the polymers. Fig. 5 shows the structure of the used PLINT TE 77 tribotester (High-Frequency Tribotest), employed by Zsidai and Kalácska in previous research [15].

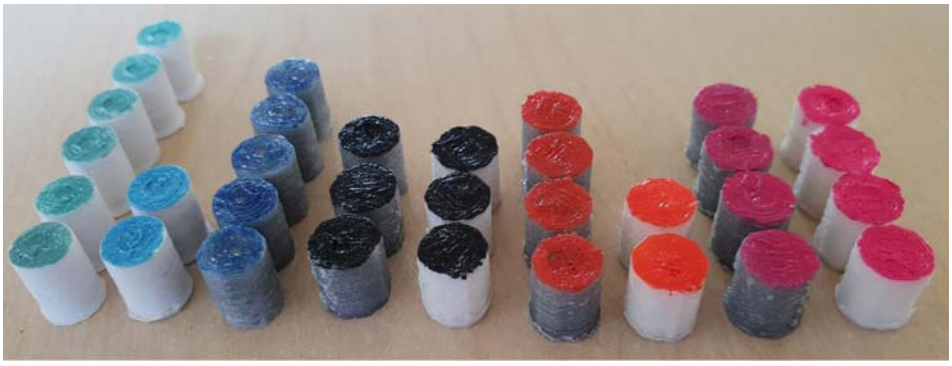

**Fig. 4.** Some of the test specimens with a colour code

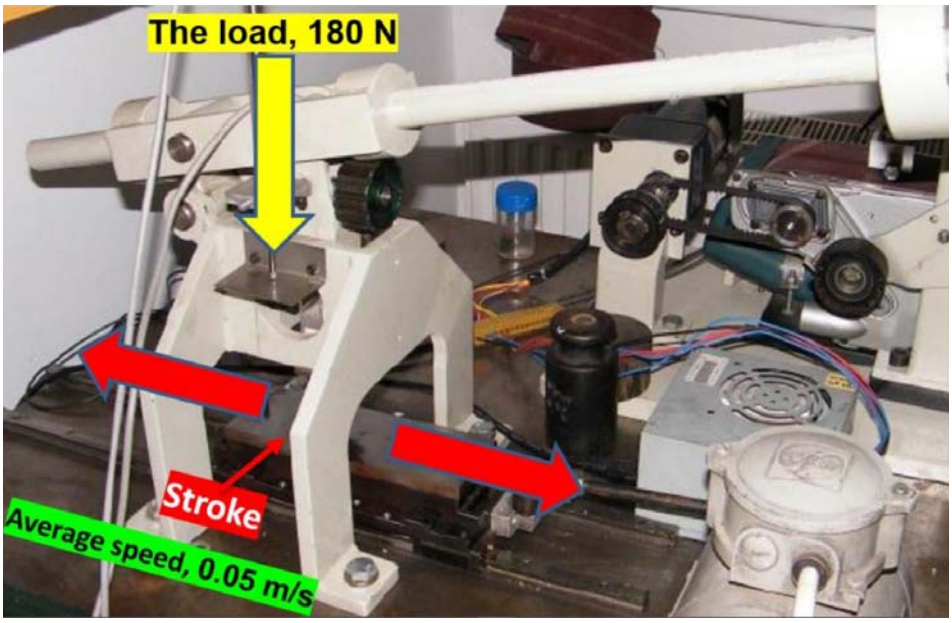


**Fig. 5.** Tribotester used for tribology test

The alternating movement required for the measurement is provided by a variable speed electric motor with an adjustable frequency drive and an eccentric disc. This eccentric disc is coupled with an interchangeable push rod by the sliding plate on the linear guides. The frequency inverter can be used to set the measurement frequency to the desired value accurately. With the eccentricity of the thrust bar, the stroke length can be adjusted according to the measurement parameters. The method for testing is a reciprocating linear sliding friction measurement without lubricants. The sliding friction is created by a polymer cylinder, which is moved against a steel plate in a counterformal contact. The polymer cylinder is clamped in a grapple and does not turn away during the test. During the current measurement, the test specimen is subjected to a static load. The loading force can be adjusted by selecting and positioning the load weights on the load arm. To measure the friction force and other essential features, various sensors in the measuring system are required. Hence, the system can measure static force, friction force, compression force along two coordinates, displacement along three coordinates, and ambient temperature. Clamping heads were used for fixing the specimen. The parallel clamping jaws were clamped by two screws provided. The clamping feature is characterised by a small movement that allows parallel rotation of the shaft to ensure the self-alignment of the body during the test. Thus, the specimen is equally laid on the steel counterpart, avoiding the possibility of wear and misalignment and minimising the probability of inaccurate measurement. Before starting the measurement, some parameters must be defined which are given in Table 3.

**Table 3.** Steel counterpart parameters

| | |
|---|---|
| Surface roughness of steel counterpart, *Rz* [μm], *Ra* [μm] | 3.2 |
| Test duration, *t* [s] | 130 |
| Load, *F* [N] | 180 |
| Alternating motion frequency, *f* [Hz] | 10 |
| Average speed, *v* [m/s] | 0.05 |
| Stroke length, [mm] | 15 |
| Relative humidity, *Rh* [%] | 50 |

The examinations were carried out under constant environmental conditions. Based on previous measurements, the duration and load of the measurements were accomplished. These parameters were suitable for determining the goals of the current work.

## 3. Results and discussion

The wear rate and the friction force are the most critical values obtained for this study. The friction force is represented by the sliding distance and determined per cycle as shown in Fig. 6. The upper curve in the figure is very dense which is not suitable for extracting understood data. Therefore, the two values from the curve between each inflexion point have been extracted. This method is illustrated in the middle part of the figure. Picking up two short areas from the whole sliding distance is to grasp the attitude of the coefficient of friction. The front and end cycles were selected for this purpose. The maximum value and an average of the steady state are representing the static and dynam-

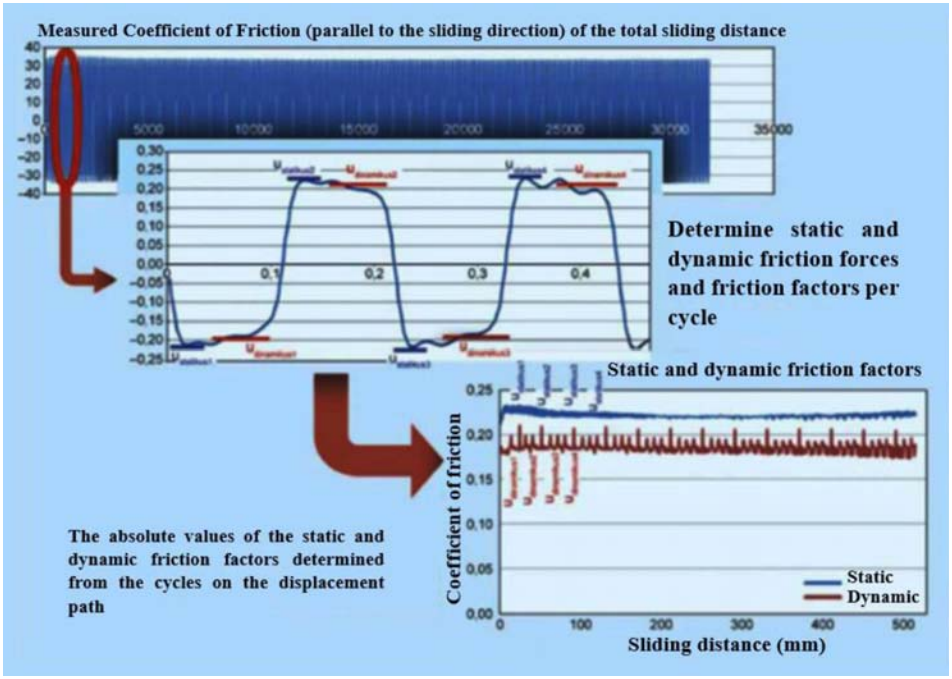


**Fig. 6.** Interpretation of measurement data

ic friction coefficients respectively. The results in the lower curves show the static and dynamic friction coefficients as a function of the displacement path.

During the test, both static and dynamic friction factors were evaluated. The value of static friction factors is always higher than the relative dynamics. A number of measurements with the given materials have been done, and the most distinctive ones are presented in the following sections.

### *3.1. PLA test result of 3d printing*

As it is mentioned in section 2.2., the PLA workpieces printed in white and grey colours. Three temperature ranges; low, opt, and max were used for each colour. Precisely the low: 190-195 °C, opt 200-205 °C, and max: 215-220 °C. The measurements were repeated on five samples for every specific setting. Regarding the friction factor, after the initial fluctuation, the coefficient of friction is set to a value which is known as the static friction factor. The static friction factor is followed closely by the value of the dynamic factor throughout the measurement time. Typically, there is a value taken by both curves named difference, which is visible on the green curve in the Figs. 7 and 11.

#### 3.1.1. White colour PLA

Figure 7 shows the static and dynamic friction factors of the 3D printed PLA in white colour at the low-tem-

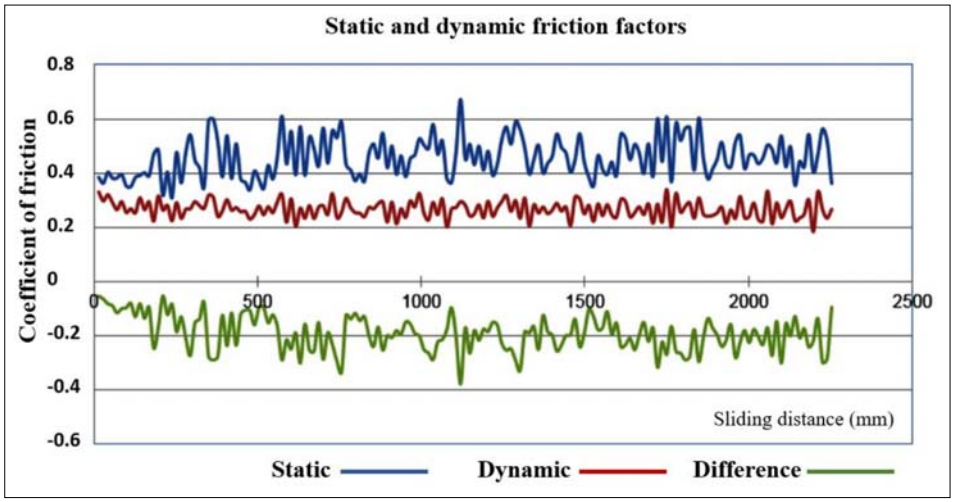


**Fig. 7.** Friction factors of the white PLA specimens which printed at low-temperature range

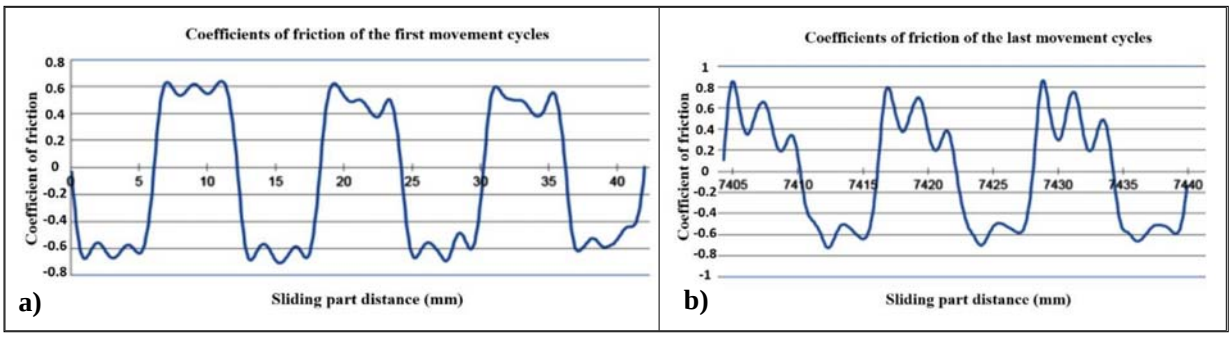


**Fig. 8.** Magnified cycles of white PLA printed at opt temperature: (a) movement beginning and (b) end movement

perature range. During the measurement, the curve moves around the same extent with a large amplitude. The curve of the difference was drawn inverted for better legibility. It can be seen that there are great jumps between the two curves during the measurement. The distinction is shown in Fig. 8 (a and b) refers to the tendency of adhesion that significantly increased at the end cycle of a workpiece printed at opt temperature. The wear of the low-temperature range samples is demonstrated in Fig. 9. It is generally characterised by a small wear value. The blue curve belongs to the first test piece measuring, where specimen surface melting has taken place. A rather intense sound effect has been recognised during the measurement. This occurs at switching the tribotester on, then leads into changing the intensity. This workpiece did not leave any significant deposits on the steel counterpart.

Because the static and dynamic friction factors of the opt and max temperature range specimens showed no different results, therefore, they are discussed without displaying their curves. These workpieces behaved like low-temperature range ones. The curve of the difference is surrounded by a high amplitude but constant range. The wear curves of these specimens (opt and max) are shown in Fig. 10. The green curve belongs to the max temperature range specimen, where it can be seen a notable deviation. The extent of the curve

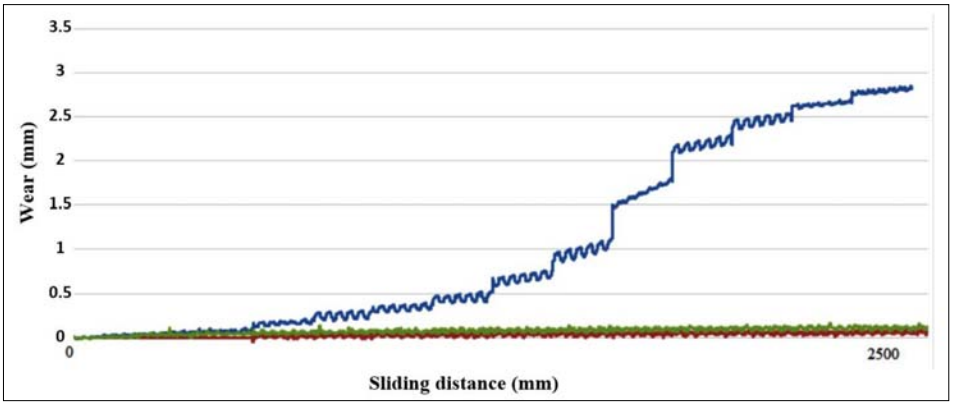


**Fig. 9.** The wear curves of three repeated tests of white PLA, printed at the low-temperature range

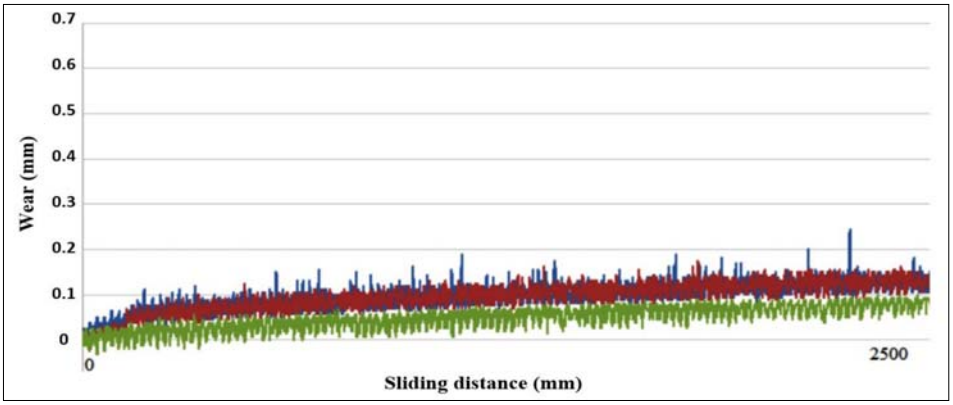


**Fig. 10.** The wear curves of three repeated tests of white PLA, printed at opt and max temperature ranges

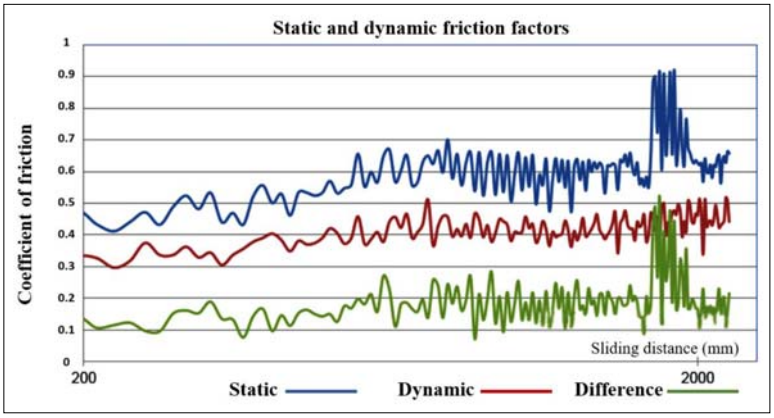


**Fig. 11.** Friction factors of the grey PLA specimens which printed at the low-temperature range

detects a big fall due to the scheduled pauses of measurement. All the measurements were accompanied by a sharp banging sound that in some cases became pulsating in the second half of the test. On the other hand, no significant deposits were left on the steel counterpart.

3.1.2. Grey colour PLA

During the measurement, the grey colour PLA specimens did not show divergence according to their manufacturing settings. Fig. 11 reveals the static and dynamic friction coefficients of low-temperature range workpiece. The static friction force sharply increased at the end of the curve. This is also seen by the difference curve. The same phenomenon appeared in the other temperature range pieces (opt and max), with different intensity. This trend can be interpreted as the indicator of melting and adhesion. The Fig. 12 (a and b) belong to an opt test, which gives the most typical values. The wear curves illustrated in Fig. 13 are representing specimens printed in diverse temperature range; the green curve is low, blue and red are opt, and violet is max. Only the max was up to the end of the measurement period. At each of the measurements, loud noise sound appeared, but it dropped quite quickly.

*3.2. ABS test result of 3d printing*

The measurement curve of the static and dynamic friction factors of the 3D printed ABS did not show an attractive outcome. The static and the dynamic curves do not typically coincide. The value of the difference curve between the two curves is almost constant. There was no distinctive sound effect heard dur-

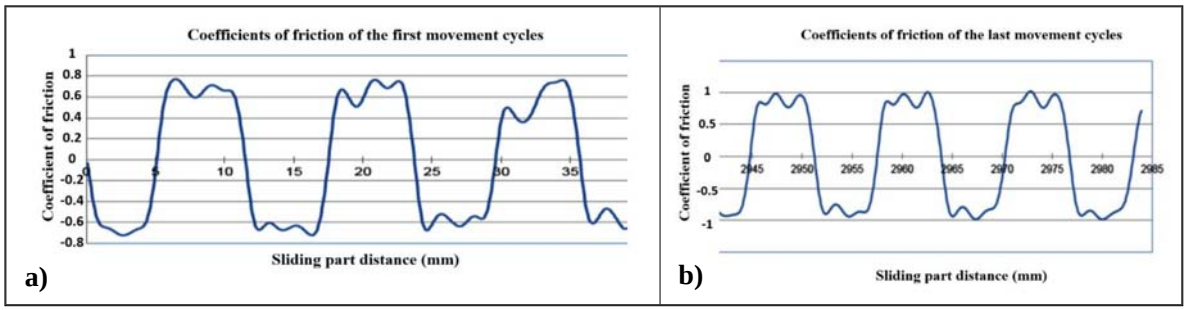


**Fig. 12.** Magnified cycles of grey PLA printed at opt temperature: (a) movement beginning and (b) end movement

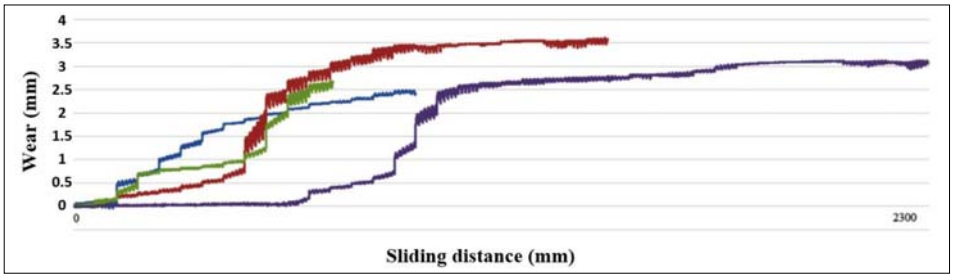


**Fig. 13.** The wear curves of four repeated tests of grey PLA, printed at low, opt, and max temperature ranges

ing the measurement. Along the measuring time, the curves tendency does not show any significant difference. The wear rate, as well as the dynamic friction of the 3D printed ABS specimens are illustrated and compared with PLA results in the comparison section.

### *3.3. Comparison of results*

Figure 14 shows the maximum and most frequent values of the dynamic friction coefficient. The dark column indicates the friction coefficient of the stabilised state, while the maximum friction value during the measurement period is illustrated by the clear supplementary column. The values appear here are from the average of multiple measurements. From the diagram, it is clear that the dynamic friction coefficient of the ABS-based specimen is less than others whether the max or stability. Regarding PLA, it can be seen that in white colour, the dynamic stability values have almost the same range regardless of the print settings. The dynamic max changes in a limited range. What had an interesting turn during the measurement and the results, are clearly shown in the coloured specimens. The grey filament values are much higher than those of white. These specimens melted during the measurement without exception.

In Fig. 15, the average wear values of the specimens during the measurement were compared. Values for *y* axis are in millimetres. For PLA, it is noticed that grey filaments are significantly worn out. However, because of melting in some of the white PLA tests, the measurement time has not gone through and had to be stopped. For instance, the low-temperature range specimen is melted. Thus, the dark column rep-

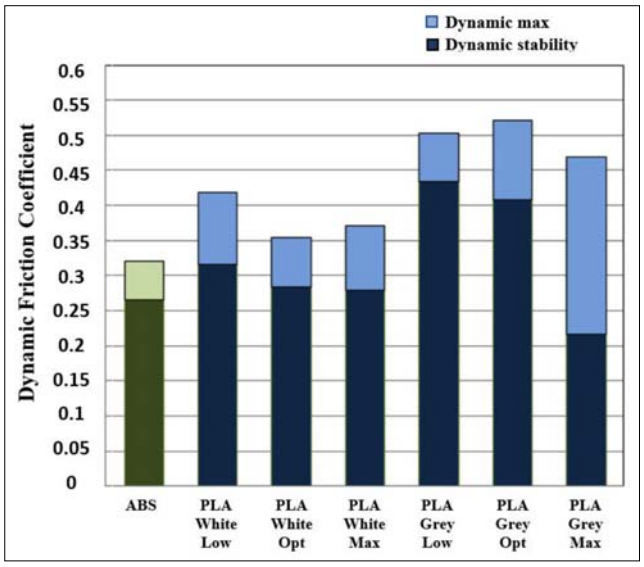


**Fig. 14.** Measurement data of the dynamic friction coefficient

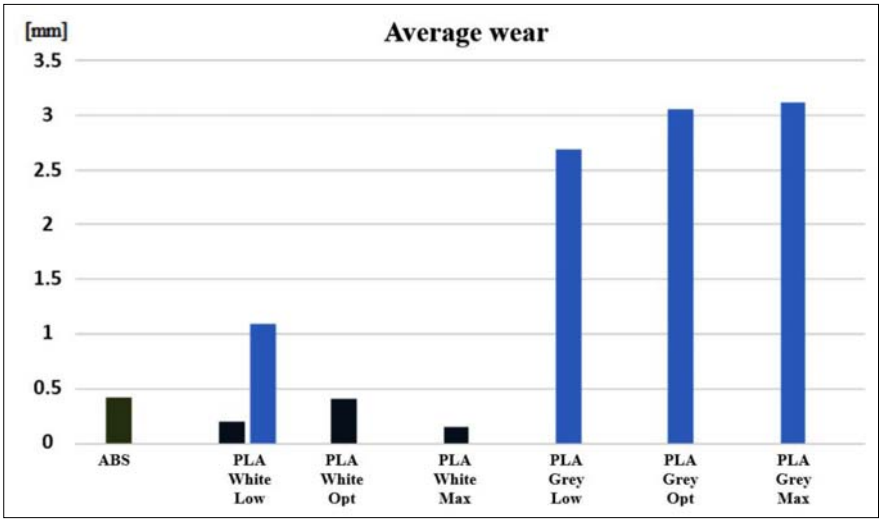


**Fig. 15.** Comparison of the average wear

resents the average of the test pieces worn through the full measurement time. Whereas, the light column indicates the shortened measurement average (the values of the measurement that are stopped earlier in this set "white PLA" because of the high degree of wear). Considering all of these, it can be concluded that the wear levels of the white PLA are somewhat lower than the ABS, but it tends to melt.

## 4. Conclusion and summary

This research aims to obtain tribological properties of different 3D printable filaments, including the determination of the difference between static and dynamic friction factors and the examination of wear values. In the light of these findings, it will be concluded with a statement on the effect of the 3D printing parameters on the tribological property. Based on the alternating-motion experiments carried out on the cylindrical plastic flat plate pairs used in this investigation, the following can be drawn:

- The alternating-motion system used through the research allows to measure the difference between static and dynamic friction factors and wear curves, so it is suitable for comparative tests of this type.
- The differences in the white ABS and PLA materials are considered to be variations in the properties of the raw materials.
- The 3D printing with the various settings tested showed some discrepancies, but they did not show a clear tendency to draw a conclusion.
- PLA specimens which are printed by the same technology, but with different colour materials, exhibited a considerable distinction.

The research on this topic can be further developed in many ways. It would be worthwhile to carry out further research on the effect of the colourants on the properties of the workpieces. It would also be an impressive area to perform a comparative examination of other material properties while looking for technological differences. Research could be extended to include mechanical tests (e.g., tensile strength) and material science measurements (e.g., hardness).

**Acknowledgements**

This work was supported by the Stipendium Hungaricum Programme and by the Mechanical Engineering Doctoral School, Szent István University, Gödöllő, Hungary.

**References**

[1] Zhang J., Xiao P. (2018), 3D printing of photopolymers. Polymer Chemistry, 9, 1530–1540. DOI: 10.1039/C8PY00157J

[2] Wang X., Jiang M., Zhou Z., Gou J., Hui D. (2017), 3D printing of polymer matrix composites: A review and prospective. Composites Part B: Engineering, 110, 442–458. DOI: 10.1016/j.compositesb.2016.11.034

[3] Ligon S. C., Liska R., Stampfl J., Gurr M., Mülhaupt R. (2017), Polymers for 3D Printing and Customized Additive Manufacturing. Chemical Reviews, 117, 10212–10290. DOI: 10.1021/acs.chemrev.7b00074

[4] Turner B. N., Strong R., Gold S. A. (2014), A review of melt extrusion additive manufacturing processes: I. Process design and modeling. Rapid Prototyping Journal, 20, 192–204. DOI: 10.1108/RPJ-01-2013-0012

[5] Sun Q., Rizvi G. M., Bellehumeur C. T., Gu P. (2008), Effect of processing conditions on the bonding quality of FDM polymer filaments. Rapid Prototyping Journal, 14, 72–80. DOI: 10.1108/13552540810862028

[6] Tran P., Ngo T. D., Ghazlan A., Hui D. (2017), Bimaterial 3D printing and numerical analysis of bio-inspired composite structures under in-plane and transverse loadings. Composites Part B: Engineering, 108, 210–223. DOI: 10.1016/j.compositesb.2016.09.083

[7] Garcia C. R., Correa J., Espalin D., Barton J. H., Rumpf R. C., Wicker R., Gonzalez V. (2012), 3D printing of anisotropic metamaterials. Progress in Electromagnetics Research Letters, 34, 75–82. DOI: 10.2528/PIERL12070311

[8] Tymrak B. M., Kreiger M., Pearce J. M. (2014), Mechanical properties of components fabricated with open-source 3-D printers under realistic environmental conditions. Materials and Design, 58, 242–246. DOI: 10.1016/j.matdes.2014.02.038

[9] Takezawa A., Kobashi M. (2017), Design methodology for porous composites with tunable thermal expansion produced by multi-material topology optimization and additive manufacturing. Composites Part B: Engineering, 131, 21–29. DOI: 10.1016/j.compositesb.2017.07.054

[10] Sidambe A. T. (2014), Biocompatibility of advanced manufactured titanium implants-A review. Materials, 7, 8168–8188. DOI: 10.3390/ma7128168

[11] Bhushan B. (2013), Principles and Applications to Tribology. UK: John Wiley & Sons, Ltd. ISBN: 9781118403020

[12] Zsidai L., De Baets P., Samyn P., Kalacska G., Van Peteghem A. P., Van Parys F. (2002), The tribological behaviour of engineering plastics during sliding friction investigated with small-scale specimens. Wear, 253, 673–688. DOI: 10.1016/S0043-1648(02)00149-7

[13] Velleman N. V., 3D Printer K8200. [Online]. Available: http://www.k8200.eu/specs/. [Accessed: 18-Oct-2018].

[14] Esun S. E. I. C. L., 3D filament PLA white. [Online]. Available: http://www.esun3d.net. [Accessed: 18-Oct-2018].

[15] Zsidai L., Kalácska G. (2014), 'Stick-slip' PA és PEEK kompozitok súrlódásánál henger/sík modell vizsgálati rendszerben. Műanyag és Gumi, 51, 462–470.